

# Redefining the Histone Deacetylase Inhibitor Pharmacophore: High Potency with No Zinc Cofactor Interaction

Douglas C. Beshore,<sup>\*,∇</sup> Gregory C. Adam, Richard J. O. Barnard, Christine Burlein, Steven N. Gallicchio, M. Katharine Holloway, Daniel Krosky, Wei Lemaire, Robert W. Myers, Sangita Patel, Michael A. Plotkin, David A. Powell, Vanessa Rada, Christopher D. Cox, Paul J. Coleman, Daniel J. Klein,<sup>\*</sup> and Scott E. Wolkenberg



Cite This: *ACS Med. Chem. Lett.* 2021, 12, 540–547



Read Online

ACCESS |



Metrics & More



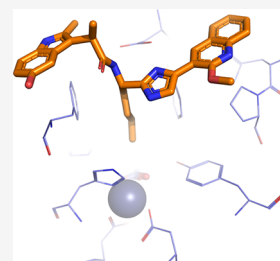
Article Recommendations



Supporting Information

**ABSTRACT:** A novel series of histone deacetylase (HDAC) inhibitors lacking a zinc-binding moiety has been developed and described herein. HDAC isozyme profiling and kinetic studies indicate that these inhibitors display a selectivity preference for HDACs 1, 2, 3, 10, and 11 via a rapid equilibrium mechanism, and crystal structures with HDAC2 confirm that these inhibitors do not interact with the catalytic zinc. The compounds are nonmutagenic and devoid of electrophilic and mutagenic structural elements and exhibit off-target profiles that are promising for further optimization. The efficacy of this new class in biochemical and cell-based assays is comparable to the marketed HDAC inhibitors belinostat and vorinostat. These results demonstrate that the long-standing pharmacophore model of HDAC inhibitors requiring a metal binding motif should be revised and offers a distinct class of HDAC inhibitors.

**KEYWORDS:** HDAC inhibitor, zinc binding, pharmacophore, HIV latency



Histone deacetylases (HDACs) are an important family of epigenetic regulatory enzymes that selectively remove  $\epsilon$ -N-acetyl groups from lysine residues of post-translationally modified proteins. In the context of histones, HDACs serve as epigenetic erasers and effect changes in the transcription of many genes in response to a variety of stimuli.<sup>1</sup> Humans encode 18 HDAC isozymes, divided among five classes (I, IIa, IIb, III, and IV). Classes I, IIa, IIb, and IV are zinc metalloenzymes that share a common three-dimensional structure, while class III HDACs, also known as sirtuins, have distinct structures unrelated to the former and possess NAD-dependent enzymatic activity.

Therapeutic inhibition of HDACs has been pursued for decades broadly across the family and selectively among subsets of the human isozymes. To date, five HDAC inhibitors (HDACis) have been approved for treatment of cutaneous and peripheral T-cell lymphoma and multiple myeloma.<sup>2,3</sup> More recently, HDAC inhibition has been evaluated clinically as a mechanism to reactivate HIV gene expression in latently infected immune cells as part of a viral eradication strategy,<sup>4–6</sup> and it has been studied preclinically in a variety of cardiovascular and neurological disease settings.<sup>7,8</sup>

Pharmacokinetic properties, mutagenic potential, and drug-induced liver injury have been associated with HDAC inhibitors,<sup>9–11</sup> potentially limiting the clinical utility of marketed HDACis beyond oncology indications. These liabilities have been associated with the metal binding elements present in the HDACi pharmacophore. Whether natural product-derived or synthetically designed, HDAC inhibitors

have a well-known pharmacophore with three elements that mimic natural peptide substrates (Figure 1): a metal binding motif that coordinates to the catalytic zinc, a hydrophobic linker that mimics the N-alkyl side chain of lysine, and a protein surface interacting moiety that serves as a peptide substrate recognition element. A structure-based explanation for this pharmacophore has been provided by X-ray crystal structures of substrate- and inhibitor-bound complexes in which ligands interact with surface residues, occupy the lysine tunnel, and position a metal binding moiety in proximity to the catalytic zinc where, depending on the ligand, they make either one or two inner-sphere contacts to the metal.<sup>12–14</sup>

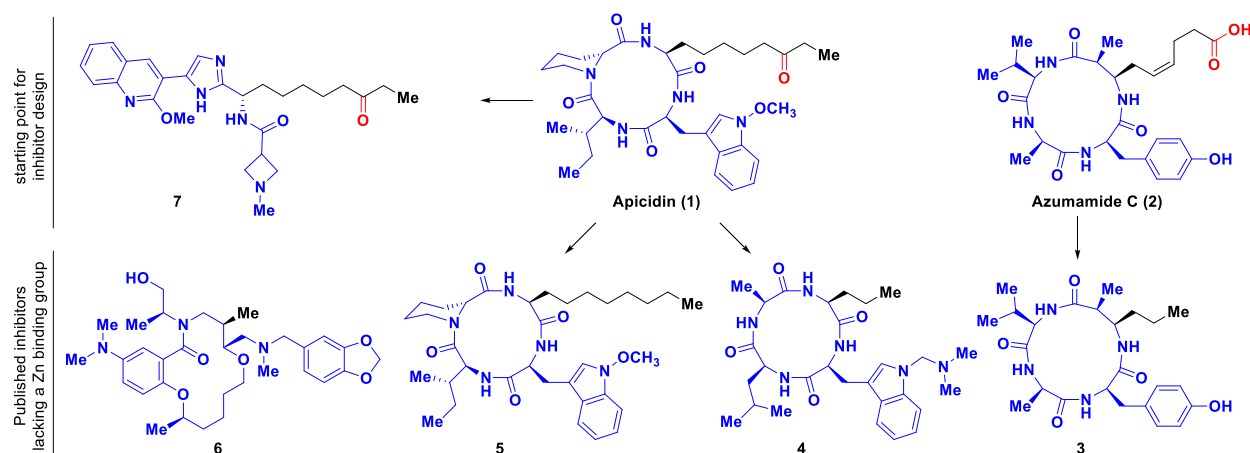
Here, we describe the discovery and optimization of highly potent HDAC inhibitors that challenge the traditional pharmacophore model by demonstrating that the previously ubiquitous metal binding motif can be removed. Without a zinc-binding moiety, these compounds do not contain electrophilic substructures (i.e., ketones), are negative in the Ames mutagenicity assay, and demonstrate cellular activity comparable to clinically utilized HDAC inhibitors. We characterized the binding mode of this novel inhibitor class

**Received:** January 31, 2021

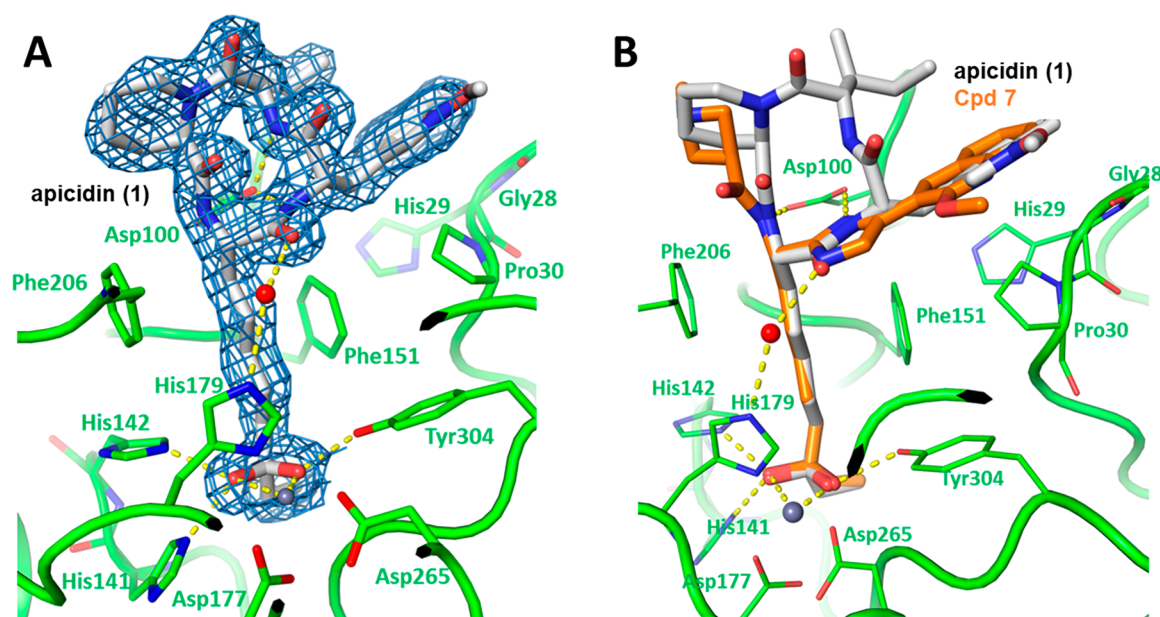
**Accepted:** February 24, 2021

**Published:** March 7, 2021





**Figure 1.** Panel of HDAC inhibitors. Natural products apicidin (1) and azumamide (2) that inspired the design of novel HDAC inhibitors that lack a zinc-binding moiety with enzymatic inhibitory activity (3–6) and apicidin-inspired ketone 7. Inhibitors are colored to indicate where they bind the HDAC active site: surface (blue), hydrophobic tunnel (black), and catalytic zinc (red).

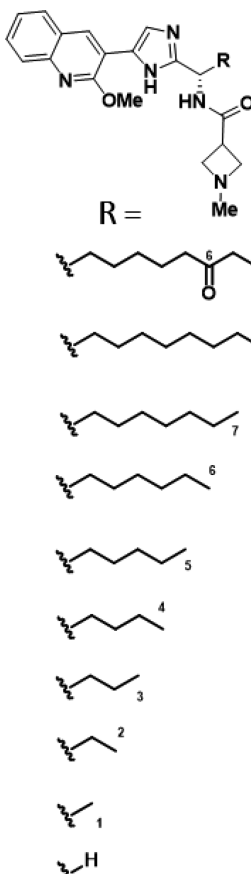


**Figure 2.** HDAC2-bound structures of apicidin (1) and compound 7. (A) Crystal structure of apicidin (1) (gray) bound to HDAC2 (green). Section of the  $2F_o - F_c$  electron density map contoured at  $1\sigma$  is overlaid (blue mesh). (B) Crystal structure of compound 7 (orange, PDB 6WBW) bound to HDAC2 (green). Apicidin 1 (gray) is overlaid for comparison. Hydrogen bonds are indicated by yellow dashes; water molecules are red spheres, and zinc is a gray sphere.

by X-ray crystallography and describe its HDAC isozyme subtype selectivity, inhibition kinetics, and activity in multiple cellular models of HIV latency reversal.

Removal of the HDACi zinc-binding moiety has been explored previously, and despite significant effort, there have only been a few compounds reported to date with measurable biochemical activity.<sup>15–18</sup> The starting points for these studies have been the natural products apicidin (1) and azumamide (2, Figure 1), which possess large, cyclic peptides that primarily interact with the protein surface. Removal of the zinc-binding elements from 1 and 2 led to inhibitors 3–5. In addition, diversity-oriented synthesis approaches identified a novel macrocyclic scaffold lacking a zinc-binding moiety (6). While each of these inhibitors exhibit significantly reduced activity in both biochemical and cellular assays, they provide inspiration that HDAC inhibition can be achieved with inhibitors that do not engage the catalytic zinc (Table S1).

To better understand the interaction network of the large cyclic peptide family of apicidins, we determined a crystal structure of apicidin (1) bound to human HDAC2 (Figure 2) and analyzed the noncovalent interactions qualitatively and quantitatively using Scorpion (Desert Scientific Software).<sup>19</sup> As observed previously in crystal structures of HDACs bound to inhibitors containing a ketone zinc-binding element,<sup>20,21</sup> the ketone of 1 is coordinated to the catalytic zinc of HDAC2 as the hydrated gem-diol(ate) making two inner-sphere contacts (Figure 2A). Although the electron density maps cannot distinguish OH from O<sup>-</sup>, we observe asymmetry in the coordination distances between the zinc and the two oxygen atoms of the gem-diol(ate) (1.9 and 2.4 Å), which is consistent with previous observations for trapoxin A, HC toxin, substrate analogs, and ketone-containing inhibitors<sup>20</sup> and suggests that nucleophilic attack by the zinc-activated water leads to a transition state mimic in which the hydroxyl (O1) is stabilized

Table 1. Structure Activity Relationships of Alkyl Chain Modifications to HDAC Inhibitors<sup>A</sup>


Compound Number	HDAC1 IC <sub>50</sub> (μM)	HDAC2 IC <sub>50</sub> (μM)	HDAC3 IC <sub>50</sub> (μM)	HDAC3 LBE	Jurkat HIV latency reversal IC <sub>50</sub> (μM) 0.1% NHS <sup>B,C</sup>
Apicidin (1)	0.001	0.009	0.002	0.27	0.12
7	0.002	0.007	0.001	0.36	0.20
8	18	>50	5.2	0.21	>40
9	Not Prepared				
10	Not Prepared				
11	4.7	>17	3.5	0.24	>40
12	0.28	0.75	0.16	0.31	17
13	0.39	3.4	0.3	0.31	11
14	23	>50	28	0.22	>40
15	>50	>50	>50	ND	>40
16	41	>50	15	0.25	>40

<sup>A</sup>Compounds tested are >95% pure as determined by LCMS and <sup>1</sup>H NMR spectra. All reported values are the mean of at least two assay measurements with standard deviation within 3-fold of the reported value. <sup>B</sup>NHS = normal human serum. <sup>C</sup>% reversal and activation are comparable across all compounds tested.

by interactions with Zn<sup>2+</sup>, His141, and His142, while the oxyanion (O2) interacts with Zn<sup>2+</sup> and Tyr304. Consistent with the network of interactions involving the zinc and nearby catalytic residues, the Scorpion scores reveal a significant contribution of the gem-diol(ate) to the overall binding of **1** (Figure S2). Moving away from the zinc-binding moiety, the methylene linker of **1** occupies the HDAC2 tunnel with most of the hydrophobic interactions involving the side chains of Phe151 and Phe206, which are conserved residues across HDAC isozymes 1, 2, and 3. The Scorpion scores for the methylene linker indicate its importance as a major contributor of favorable noncovalent interactions that drive potency. Beyond the HDAC2 tunnel, the cyclic peptide of **1** sits on the protein surface. Despite its relatively large size, the most noteworthy interactions come from just two parts of the macrocyclic peptide. First, the three amide NHs of the cyclic peptide are all within the hydrogen bonding distance of the side chain of Asp100 (Figure 2A), and the Scorpion scores for these atoms reflect these favorable contacts (Figure S2). Second, the indole of **1** is stacked on top of Gly28, His29, and Pro30. In contrast, the *iso*-leucyl and piperidinyl side chains of the cyclic peptide are solvent exposed with little direct contribution to binding. This helps explain the moderate ligand binding efficiency (LBE) of **1** (0.27), despite its interaction with the catalytic zinc.

In addition to apicidin, we considered the acyclic synthetic inhibitor **7** (Figure 1) as a starting point to evaluate the

removal of the zinc-binding motif. Compound **7** is the result of the optimization of a screening hit related to apicidin and has been previously described.<sup>22–24</sup> Compound **7** exhibits a similar profile when compared to **1**, including biochemical inhibitory potency and HDAC isozyme selectivity, and both contain a ketone zinc-binding moiety. However, **7** is smaller than **1** (478 Da vs 624 Da) and is more ligand efficient (HDAC3 ligand efficiency (LE) of 0.36 for **7**, compared to 0.27 for apicidin **1**).

We previously reported the crystal structure of **7** bound to HDAC2,<sup>25</sup> which allowed us to directly compare its binding mode to that of **1** (Figure 2B). The gem-diol(ate) zinc-binding motif and methylene linker of **7** are nearly indistinguishable from **1**, in terms of both conformation and noncovalent interactions with HDAC2. However, noteworthy differences are observed at the protein surface region due to chemical divergence of the two compounds. The quinoline of **7** occupies a similar space as the indole of **1**, making interactions with Gly28, His29, and Pro30 but with subtle differences (i.e., the methoxyethers of the two do not overlap). The imidazole and amide NHs of **7** also preserve bidentate hydrogen bonds to Asp100. Finally, the azetidine follows the same path as that of the cyclic peptide **1**, partially overlapping with the piperidinyl side chain. As judged by the extent of their noncovalent interactions, **1** and **7** are quite similar (overall Scorpion scores of 24.5 and 23.1 for **1** and **7**, respectively) with similar distributions of key contacts heavily weighted toward the zinc-binding group and linker (Figure S2). As such, we viewed **7** as

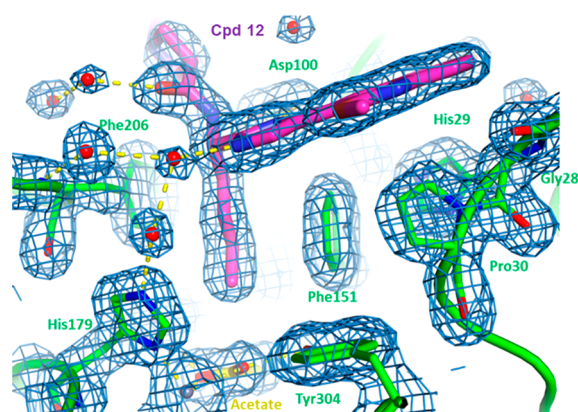


an attractive lead for identifying small molecule HDAC inhibitors lacking a zinc-binding moiety.

The exploration of structure activity relationships (SARs) of the lysine-mimicking alkyl chain was examined by removing the ketone of **7** and varying the length of the alkyl chain from zero to eight carbons (Table 1). The deletion of the carbonyl of **7** without truncation of the alkyl chain provided compound **8** and resulted in a 3–4 log loss in biochemical inhibitory potency against HDACs 1, 2, and 3. This large reduction in activity can be explained through the loss of inner-sphere zinc coordination contacts of the inhibitor and the introduction of unfavorable contacts between the nonpolar linker and the catalytic zinc. On the basis of this rationale, compounds with a shortened alkyl chain containing six or seven carbons were expected to have similarly unfavorable interactions with the catalytic zinc and were not prepared (i.e., **9** and **10**). Compounds with alkyl chains of five carbons or fewer (compounds **11**–**16**) were synthesized, and their inhibitory activity was measured. The five-carbon chain inhibitor **11** had a similar HDAC inhibition profile as compound **8**. In contrast, a significant improvement in biochemical activity was observed (nanomolar potency range) when the alkyl chain was shortened to either four or three carbon atoms, **12** and **13**, respectively. Further truncation to two, one, or no carbons (i.e., **14**–**16**) led to a gradual weakening of HDAC inhibitory activity, illustrating the importance of retaining the favorable nonpolar interactions of the alkyl chain.

Both **12** and **13** had the highest HDAC3-derived ligand binding efficiency in this set and demonstrated measurable, albeit weak, activity in a cellular model of HIV latency reversal.<sup>26</sup> However, the relative potency of compound **12** across HDACs 1, 2, and 3 revealed a more balanced profile when compared to **13** that was similar to its progenitors **1** and **7**. These data demonstrated that a similar degree of pan-inhibition can be achieved against the class I HDAC isozymes in the absence of a zinc-binding moiety. Importantly, **12** was found to be Ames-negative in an exploratory non-GLP 3-strain Ames assay. The selectivity profile of inhibitor **12** against HDACs 1–11 was examined in a panel of enzymatic assays, revealing that **12** was quite selective for HDACs 1, 2, 3, and 10 (Table S3).

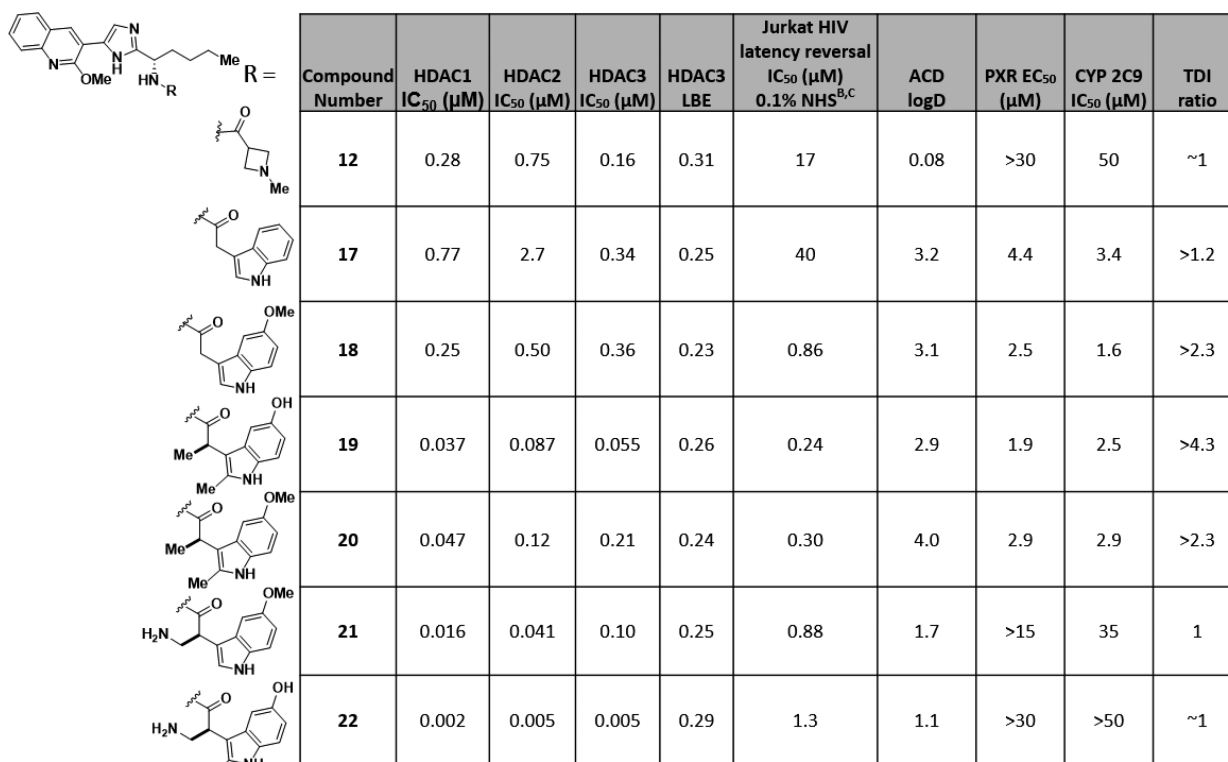
The X-ray crystal structure of **12** bound to HDAC2 reveals clear electron density for the inhibitor in a binding pose that does not interact with the catalytic zinc (Figure 3). Shared



**Figure 3.** Crystal structure of compound **12** (magenta) bound to HDAC2 (green). The  $2F_o - F_c$  electron density is shown (blue mesh), contoured at  $1\sigma$ .

structural elements of **7** and **12** show indistinguishable ligand conformations in their respective HDAC2-bound states, and the binding pocket residues adopt the same conformation. Rather than contacting inhibitor **12**, the catalytic zinc is bound instead to an acetate buffer ion through bidentate inner-sphere contacts; the interaction of a zinc-bound acetate has been observed in other inhibitor-free crystal structures of HDAC isozymes.<sup>27,20,28</sup> The acetate is also within the van der Waals interaction distance of the terminal methyl of **12** in the HDAC2 tunnel. A key observation made from the HDAC2 cocrystal structure with **12** is that the linker length is sufficient to capture available hydrophobic contacts with the side chains of Phe151 and Phe206. Therefore, the >100-fold loss of potency observed for inhibitor **12** is ascribed to the loss of the interaction made by the hydrated ethyl ketone with the catalytic zinc.

With the four-carbon alkyl chain of **12** providing submicromolar inhibitory potency and desirable ligand efficiency, we turned next to optimization of the ligand–protein surface interactions. The replacement of the azetidinyamide was prioritized because few protein–ligand interactions were observed with the azetidine (Figures 2B and 3), providing little contribution to the Scorpion scores of compounds **7** and **12** (Figure S4). An unbiased library approach was taken, which led to the identification of the indole acetamide **17** (Table 2). While simple indoles have been shown to be suitable azetidine replacements for inhibitors that contain zinc-binding moieties,<sup>22,23</sup> the efforts described herein focused on improving activity in the absence of the zinc-binding moiety. This led to divergent SAR with additional elaboration of the indole moiety proving to be key to unlocking highly potent HDAC inhibitors (Table 2). Initial libraries revealed that indole **17** and 5-methoxyindole **18** were able to provide similar relative potency profiles as **12** with balanced HDACs 1, 2, and 3 inhibition. However, replacement of the azetidine resulted in inhibitors with lower ligand efficiency that were significantly more lipophilic (i.e., ACD LogP), leading to increased off target activities including PXR activation, reversible CYP450 inhibition, and time-dependent CYP3A4 inhibition (TDI) (Table 2). Indole substitution at the 2-position and the introduction of a methyl to the benzylic methylene led to compounds **19** and **20**, which showed improvement in inhibitory potency while maintaining a HDAC3 LBE of 0.25. HDAC panel selectivity was examined for **19**, revealing a similar profile to **12** with selectivity for HDACs 1, 2, 3, 10, and 11 (Table S3). Both **12** and **19** possessed overall HDAC selectivity profiles similar to vorinostat. Compound **19** exhibited good selectivity in a lead profiling panel of 115 biochemical and binding assays at Eurofins Panlabs, Inc., designed to study its selectivity beyond the HDAC enzyme family. The panel consisted of a wide variety of receptors, enzymes, and transporters. The compound was tested in duplicate at 10  $\mu\text{M}$ . Significant hits, defined as showing >50% effect at 10  $\mu\text{M}$ , were subsequently titrated. Compound **19** was found to have one significant hit, which titrated to <1  $\mu\text{M}$  (binding to human serotonin 5-HT<sub>2B</sub> receptor), and 9 hits titrating between 1 and 10  $\mu\text{M}$ . This represents selectivity of 10–1000-fold for HDAC inhibition and suggests that **19** is a promising lead for further optimization (Table S5). Additionally, compound **19** was negative in the exploratory Ames assay and exhibited reasonable pharmacokinetic properties ( $\text{Cl}_p$  25 mL/min/kg,  $t_{1/2}$  1.2 h, F 26%, Wistar Han rats).

Table 2. Structure Activity Relationships of Indole Acetamide HDAC Inhibitors<sup>A</sup>


Compound Number	HDAC1 IC <sub>50</sub> (μM)	HDAC2 IC <sub>50</sub> (μM)	HDAC3 IC <sub>50</sub> (μM)	HDAC3 LBE	Jurkat HIV latency reversal IC <sub>50</sub> (μM) 0.1% NHS <sup>B,C</sup>	ACD logD	PXR EC <sub>50</sub> (μM)	CYP 2C9 IC <sub>50</sub> (μM)	TDI ratio
12	0.28	0.75	0.16	0.31	17	0.08	>30	50	~1
17	0.77	2.7	0.34	0.25	40	3.2	4.4	3.4	>1.2
18	0.25	0.50	0.36	0.23	0.86	3.1	2.5	1.6	>2.3
19	0.037	0.087	0.055	0.26	0.24	2.9	1.9	2.5	>4.3
20	0.047	0.12	0.21	0.24	0.30	4.0	2.9	2.9	>2.3
21	0.016	0.041	0.10	0.25	0.88	1.7	>15	35	1
22	0.002	0.005	0.005	0.29	1.3	1.1	>30	>50	~1

<sup>A</sup>Compounds tested are >95% pure as determined by LCMS and <sup>1</sup>H NMR spectra. All reported values are the mean of at least two assay measurements with standard deviation within 3-fold of the reported value. <sup>B</sup>NHS = normal human serum. <sup>C</sup>% reversal and activation are comparable across all compounds tested.

On the basis of our understanding of the binding conformation of compound 12, we hypothesized that the indolyl–methyl of 19 provided a favorable conformational bias, positioning the indole to interact with the protein surface. While the methyl does contribute to increasing potency, it does so at the expense of projecting a lipophilic substituent into bulk solvent, thus simultaneously imposing an unfavorable entropic penalty. We determined a crystal structure of 19 bound to HDAC2 (Figure 4), which confirmed both the conformation of the substituted indole and the solvent exposure of the methyl substituent. In order to mitigate the entropic penalty, an aminomethylene was incorporated in place of the methyl group, resulting in further potency enhancement while maintaining ligand efficiency and simultaneously improving the physicochemical properties (compound 21). When the aminomethylacetamide was combined with a hydroxyl at the 5-position of the indole, inhibitor 22 was discovered. Despite lacking a zinc-binding moiety, 22 achieves comparable ligand efficiency and biochemical potency against HDACs 1, 2, and 3 as progenitors 7 and 1, which contain zinc-binding elements that contribute significantly to their HDAC potencies. Moreover, compound 22 and related molecules in this series have lowered ACD LogD and reduced off-target activities, providing the first proof-of-concept that HDAC inhibitors with low nanomolar potency are possible without interacting with the catalytic zinc.

To understand the kinetic properties of inhibitors in this series, compounds 7, 12, and 19 were selected because they represent a range of IC<sub>50</sub>'s and allow a kinetic comparison of molecules with and without a zinc-binding moiety. The three compounds were examined for the inhibition of HDAC3 using

progress curve analysis. Consistent with ketone 7 and previously reported HDAC inhibitors lacking a zinc-binding moiety,<sup>16–18,29</sup> compounds 12 and 19 both inhibit HDAC3 with linear progress curves indicating fast-on/fast-off kinetics (Figure S6). Jump dilution experiments performed for both 12 and 19 bound to HDAC3 corroborated a rapid dissociation mechanism for the inhibitors as the enzymatic rate rapidly recovered upon compound dilution (data not shown).

HDAC inhibition has been shown to disrupt HIV latency with several published clinical studies of marketed HDAC inhibitors (developed for oncology) showing promising results.<sup>4,6</sup> We evaluated a panel of compounds, alongside the marketed drugs belinostat and vorinostat, in HIV latency reversal assays. Two model systems were evaluated in these studies. In the first system, a latently infected Jurkat cell line<sup>26,30</sup> was used that contains a single integrated lentiviral vector expressing the Tat H13L mutant gene and a partially attenuated TAT variant as well as TAR RNA elements derived from HIV-1NL4-3. For detection, a luciferase reporter protein was inserted in place of the Nef gene. Activation of the latent HIV provirus is monitored by an increase in luminescence, resulting from the expression of the luciferase reporter. This is reported in Tables 1 and 2. In a second model system, selected inhibitors were evaluated for their effects on HIV latency in a primary cell model.<sup>30,31</sup> Naive CD4+ T cells isolated from peripheral blood mononuclear cells from healthy donors were polarized and infected with VSV-G pseudotyped HIV-1 lacking GagPol but containing Tat H13L, Env, CD8a, and Nef. As a reporter of viral expression, Nanoluciferase P (Nluc) was inserted downstream of IRES. Post-infection, CD8a positive cells were selected and then driven to quiescence by reducing

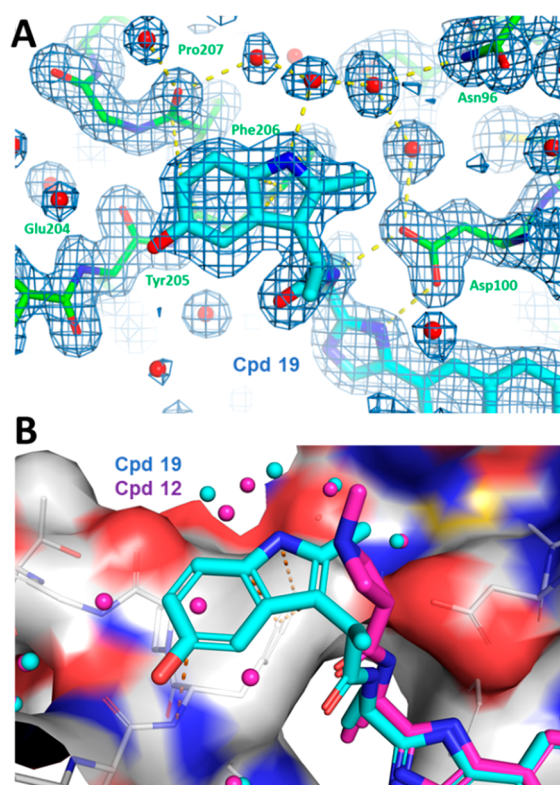


**Figure 4.** (A) Crystal structure and electron density map (blue mesh, contoured at  $1\sigma$ ) for compound **19** containing a hydroxy-methyl-indole. Edge–Face  $\pi$  electron interactions and an extensive water network mediating protein–ligand interaction are observed. (B) Overlay of **19** (cyan) and **12** (magenta). Water molecules are depicted as spheres and the protein, as a semitransparent surface.

cytokines in cell media. After 28 days post-isolation, cells were monitored for quiescence by reduction in Nluc activity and  $K_{i-67}$ . Quiescent cells were treated with compounds for 24 h and then monitored for reactivation from latency by monitoring the expression of the nanoluciferase reporter via the addition of the NanoGlo luminescent substrate.

Activities in the Jurkat cell latency reversal, primary T-cell model, and biochemical HDAC3 inhibition assays are shown in Table 3. Human serum (NHS) concentrations were varied in the media for the Jurkat latency reversal assay (0.1% and 5% NHS), and the primary T-cell model was conducted in the presence of 10% fetal bovine serum (FBS). Marketed

hydroxamic acid-based HDAC inhibitors vorinostat and belinostat, both of which have been evaluated for HIV latency reversal in a clinical setting, show similar activity across these cellular models of HIV reversal. Their efficacy was unaffected by assay serum concentrations due to their large unbound fractions in rat plasma. Ketone-based HDAC inhibitors apicidin (**1**) and **7** were also effective in these cellular models of HIV reactivation with apicidin demonstrating significant shifts between 0.1%, 5%, and 10% serum concentrations, attributable to its high plasma protein binding. Gratifyingly, the novel inhibitors **19**, **21**, and **22**, which lack a Zn-binding group, all demonstrated cellular activity in both models of HIV reactivation. In the T-cell model, **19**, **21**, and **22** showed comparable activity (2–5  $\mu\text{M}$ ) to clinically utilized HDAC inhibitors vorinostat and belinostat, apicidin (**1**), and compound **7**. Consistent with cellular activity being impacted by serum levels, the  $\text{IC}_{50}$  of **19** shifts 10-fold higher between 0.1% and 5% serum in the Jurkat model and has a similar potency in the primary T-cell assay. Similarly, inhibitors **21** and **22** have large shifts attributable to the presence of serum and their high plasma protein binding. This provides a plausible rationale for the observed biochemical to cellular shifts across the HDAC inhibitors evaluated herein, suggesting that further optimization of cellular activity could be achieved through improvements in the physicochemical properties of leads **19**, **21**, and **22**. Taken together, the activity of the non-zinc binding HDAC inhibitors described herein represents a significant advance to the field, redefining the basic understanding of the requirements needed for a potent small molecule HDACi. These serve as attractive leads for further evaluation and as different tools for continued evaluation of HDACis as latency reversal agents.

HDAC inhibitors have proven their utility in an oncology setting and recently have shown utility in HIV latency reversal. As such, there is a need to address the limitations of this important class of biologically active molecules. A novel series of HDAC inhibitors lacking a zinc-binding moiety has been developed and described herein. The class of inhibitors described herein do not interact with the catalytic zinc and are nonmutagenic, devoid of electrophilic and mutagenic structural elements. This newly disclosed HDAC inhibitor class exhibits promising selectivity profiles with biochemical and cell-based efficacy comparable to the marketed HDAC inhibitors belinostat and vorinostat.

**Table 3.** Biochemical and Cellular Activity of Selected Compounds in Cellular Models of HIV Latency Reversal<sup>A</sup>

compound	HDAC3 $\text{IC}_{50}$ (nM)	fraction unbound in rat plasma	Jurkat HIV latency reversal $\text{IC}_{50}$ ( $\mu\text{M}$ ) 0.1% NHS <sup>B,D,E</sup>	Jurkat HIV latency reversal $\text{IC}_{50}$ ( $\mu\text{M}$ ) 5% NHS <sup>B,D,E</sup>	primary T-cell model $\text{IC}_{50}$ ( $\mu\text{M}$ ) 10% FBS <sup>C,D,E</sup>
vorinostat	29 $\pm$ 13	0.75	1.6 $\pm$ 0.2	1.9 $\pm$ 0.3	2.0 $\pm$ 0.7
belinostat	7.3 $\pm$ 2	0.138	0.47 $\pm$ 0.001	0.62 $\pm$ 0.02	1.3 $\pm$ 0.2
apicidin ( <b>1</b> )	1.7 <sup>F</sup>	0.0045	0.12 <sup>F</sup>	0.59 <sup>F</sup>	5.4 <sup>D,F</sup>
<b>7</b>	0.6 $\pm$ 0.03	0.0574	0.30 $\pm$ 0.02	1.0 $\pm$ 0.02	0.71 $\pm$ 0.3
<b>19</b>	55.2 $\pm$ 20.5	0.0006	0.24 $\pm$ 0.07	3.2 $\pm$ 0.4	2.1 $\pm$ 0.03
<b>21</b>	18 <sup>F</sup>	<0.0001	1.0 $\pm$ 0.2	4.8	2.3 $\pm$ 0.08
<b>22</b>	4.7 $\pm$ 2.0	<0.0001	1.3 <sup>F</sup>	7.4	4.5 $\pm$ 0.2

<sup>A</sup>Compounds tested are >95% pure as determined by LCMS and <sup>1</sup>H NMR spectra. All reported values are the mean of at least two assay measurements with standard deviation within 3-fold of the reported value. <sup>B</sup>NHS = normal human serum. <sup>C</sup>FBS = fetal bovine serum. <sup>D</sup>reversal and activation is comparable across all compounds tested. <sup>E</sup> $\text{IC}_{50}$  determination was determined in the presence of an  $\text{EC}_{10}$  of vorinostat. <sup>F</sup> $n = 1$ .



## ■ ASSOCIATED CONTENT

### Supporting Information

The Supporting Information is available free of charge at <https://pubs.acs.org/doi/10.1021/acsmchemlett.1c00074>.

Comparison of lead compound **13** to published HDAC inhibitors, Scorpion scores for compounds, HDAC isozyme selectivity of select inhibitors, summary of significant hits for **19**, X-ray crystallography, CYP3A4 induction assay, CYP2C9 reversible inhibition assay, CYP3A4 time-dependent inhibition assay, HDAC kinetics, jump dilutions/biochemical characterization, HDACs 1, 2, and 3 protein expression and purification and inhibition assay methods, HDAC enzymatic assay panel at Eurofins CEREPS, HIV latency reversal assay, primary T cell assay, mutagenicity testing, compound preparation and characterization data (PDF)

### Accession Codes

Crystallographic data and coordinates for compounds **1**, **12**, and **19** have been deposited in the Protein Data Bank with accession codes 7LTG, 7LTK, and 7LTL, respectively.

## ■ AUTHOR INFORMATION

### Corresponding Authors

**Douglas C. Beshore** – MRL, Merck & Co., Inc., Kenilworth, New Jersey 07033, United States; [orcid.org/0000-0001-9746-1863](https://orcid.org/0000-0001-9746-1863); Email: [douglas\\_beshore@merck.com](mailto:douglas_beshore@merck.com)

**Daniel J. Klein** – MRL, Merck & Co., Inc., Kenilworth, New Jersey 07033, United States; Email: [daniel\\_klein@merck.com](mailto:daniel_klein@merck.com)

### Authors

**Gregory C. Adam** – MRL, Merck & Co., Inc., Kenilworth, New Jersey 07033, United States

**Richard J. O. Barnard** – MRL, Merck & Co., Inc., Kenilworth, New Jersey 07033, United States

**Christine Burlein** – MRL, Merck & Co., Inc., Kenilworth, New Jersey 07033, United States

**Steven N. Gallicchio** – MRL, Merck & Co., Inc., Kenilworth, New Jersey 07033, United States

**M. Katharine Holloway** – MRL, Merck & Co., Inc., Kenilworth, New Jersey 07033, United States

**Daniel Krosky** – MRL, Merck & Co., Inc., Kenilworth, New Jersey 07033, United States

**Wei Lemaire** – MRL, Merck & Co., Inc., Kenilworth, New Jersey 07033, United States

**Robert W. Myers** – MRL, Merck & Co., Inc., Kenilworth, New Jersey 07033, United States; [orcid.org/0000-0003-2599-1050](https://orcid.org/0000-0003-2599-1050)

**Sangita Patel** – MRL, Merck & Co., Inc., Kenilworth, New Jersey 07033, United States

**Michael A. Plotkin** – MRL, Merck & Co., Inc., Kenilworth, New Jersey 07033, United States

**David A. Powell** – MRL, Merck & Co., Inc., Kenilworth, New Jersey 07033, United States

**Vanessa Rada** – MRL, Merck & Co., Inc., Kenilworth, New Jersey 07033, United States

**Christopher D. Cox** – MRL, Merck & Co., Inc., Kenilworth, New Jersey 07033, United States

**Paul J. Coleman** – MRL, Merck & Co., Inc., Kenilworth, New Jersey 07033, United States

**Scott E. Wolkenberg** – MRL, Merck & Co., Inc., Kenilworth, New Jersey 07033, United States

Complete contact information is available at:

<https://pubs.acs.org/doi/10.1021/acsmchemlett.1c00074>

### Author Contributions

<sup>V</sup>D.C.B.: Lead contact. Designed the research: D.C.B., G.C.A., R.J.O.B., D.K., R.W.M., D.A.P., C.D.C., P.J.C., D.J.K., and S.E.W. Performed the experiments: D.C.B., G.C.A., R.J.O.B., C.B., S.N.G., D.K., W.L., R.W.M., S.P., M.A.P., V.R., and D.J.K. Analyzed the data: D.C.B., G.C.A., R.J.O.B., C.B., S.N.G., M.K.H., D.K., W.L., R.W.M., S.P., M.A.P., D.A.P., V.R., C.D.C., P.J.C., D.J.K., and S.E.W. Wrote the paper: D.C.B., G.C.A., D.J.K., and S.E.W.

### Notes

The authors declare the following competing financial interest(s): Authors are current or former employees of Merck & Co., Inc., Kenilworth, NJ, USA and potentially own stock and/or hold stock options in the Company.

### Biographies

**Douglas C. Beshore** is a Principal Scientist in the Department of Medicinal Chemistry at Merck & Co., Inc. His research interests include molecular optimization, hit-to-lead progression, and early program development with a focus in infectious disease and neuroscience drug discovery. He obtained his B.S. in Biochemistry from Albright College and his Ph.D. from the University of Pennsylvania in the laboratories of Prof. Amos B. Smith, III. He is currently based at the Merck Research Laboratories in West Point, Pennsylvania.

**Daniel J. Klein** is a Director in the Department of Computational and Structural Chemistry at Merck & Co., Inc. His research interests are in structure-based drug design and small molecule drug discovery with a focus on infectious diseases and neuroscience. Daniel received his Ph.D. in Molecular Biophysics and Biochemistry from Yale University with Professor Tom Steitz and was a Damon Runyon Postdoctoral Fellow at the Fred Hutchinson Cancer Research Center with Dr. Adrian Ferre-D'Amare. He is currently based at the Merck Research Laboratories site in West Point, Pennsylvania.

## ■ ACKNOWLEDGMENTS

X-ray diffraction data for compound **1** was collected at the Canadian Light Source. X-ray diffraction data for compounds **12** and **19** were collected at beamline 17-ID in the facilities of the Industrial Macromolecular Crystallography Association Collaborative Access Team (IMCA-CAT) at the Advanced Photon Source, Argonne National Laboratories. Use of the IMCA-CAT beamline was supported by the companies of the Industrial Macromolecular Crystallography Association through a contract with Hauptman-Woodward Medical Research Institute. Use of the Advance Photon Source was supported by the US Department of Energy, Office of Science, Office of Basic Energy Sciences, under Contract No. DE-AC02-06CH11357. The authors thank Dr. James Small for obtaining and interpreting NMR spectra and Anthony Soares for obtaining and interpreting HRMS data.

## ■ REFERENCES

- (1) Haberland, M.; Montgomery, R. L.; Olson, E. N. The many roles of histone deacetylases in development and physiology: implications for disease and therapy. *Nat. Rev. Genet.* **2009**, *10*, 32–42.
- (2) Tandon, N.; Ramakrishnan, V.; Kumar, S. K. Clinical use and applications of histone deacetylase inhibitors in multiple myeloma. *Clin. Pharmacol.* **2016**, *8*, 35–44.

- (3) Porter, N. J.; Christianson, D. W. Binding of the microbial cyclic tetrapeptide Trapoxin A to the class I histone deacetylase HDAC8. *ACS Chem. Biol.* **2017**, *12*, 2281–2286.
- (4) Margolis, D. M.; Garcia, J. V.; Hazuda, D. J.; Haynes, B. F. Latency reversal and viral clearance to cure HIV-1. *Science* **2016**, *353*, 6297.
- (5) Archin, N. M.; Keedy, K. S.; Espeseth, A.; Dang, H.; Hazuda, D. J.; Margolis, D. M. Expression of latent human immunodeficiency type 1 is induced by novel and selective histone deacetylase inhibitors. *AIDS* **2009**, *23*, 1799–1806.
- (6) Wolkenberg, S. E.; Tellers, D. M.; Converso, A.; Barnard, R. J. O. Approaches to eradicate HIV infection. In *ACS Medicinal Chemistry Reviews*, 2016; Vol 51, pp 205–225.
- (7) Li, P.; Ge, J.; Li, H. Lysine acetyltransferases and lysine deacetylases as targets for cardiovascular disease. *Nat. Rev. Cardiol.* **2020**, *17*, 96–115.
- (8) Ziemka-Nalecz, M.; Jaworska, J.; Sypecka, J.; Zalewska, T. Histone deacetylase inhibitors: a therapeutic key in neurological disorders. *J. Neuropathol. Exp. Neurol.* **2018**, *77*, 855–870.
- (9) Shen, S.; Kozikowski, A. P. Why hydroxamates may not be the best histone deacetylase inhibitors—what some may have forgotten or would rather forget? *ChemMedChem* **2016**, *11*, 15–21.
- (10) Subramanian, S.; Bates, S. E.; Wright, J. J.; Espinoza-Delgado, I.; Piekarczyk, R. L. Clinical toxicities of histone deacetylase inhibitors. *Pharmaceuticals* **2010**, *3*, 2751–2767.
- (11) Cengiz Seval, G.; Beksac, M. A comparative safety review of histone deacetylase inhibitors for the treatment of myeloma. *Expert Opin. Drug Saf.* **2019**, *18*, 563–571.
- (12) Lombardi, P. M.; Cole, K. E.; Dowling, D. P.; Christianson, D. W. Structure, mechanism, and inhibition of histone deacetylases and related metalloenzymes. *Curr. Opin. Struct. Biol.* **2011**, *21*, 735–743.
- (13) Maolanon, A. R.; Madsen, A. S.; Olsen, C. A. Innovative strategies for selective inhibition of histone deacetylases. *Cell Chem. Biol.* **2016**, *23*, 759–768.
- (14) Chen, K.; Xu, L.; Wiest, O. Computational exploration of zinc binding groups for HDAC inhibition. *J. Org. Chem.* **2013**, *78*, 5051–5055.
- (15) Colletti, S. L.; Myers, R. W.; Darkin-Rattray, S. J.; Schmatz, D. M.; Fisher, M. H.; Wyratt, M. J.; Meinke, P. T. Design and synthesis of histone deacetylase inhibitors: the development of apicidin transition state analogs. *Tetrahedron Lett.* **2000**, *41*, 7837–7841.
- (16) Marcaurrelle, L. A.; Comer, E.; Dandapani, S.; Duvall, J. R.; Gerard, B.; Kesavan, S.; Lee, M. D.; Liu, H.; Lowe, J. T.; Marie, J.-C.; Mulrooney, C. A.; Pandya, B. A.; Rowley, A.; Ryba, T. D.; Suh, B.-C.; Wei, J.; Young, D. W.; Akella, L. B.; Ross, N. T.; Zhang, Y.-L.; Fass, D. M.; Reis, S. A.; Zhao, W.-N.; Haggarty, S. J.; Palmer, M.; Foley, M. A. An aldol-based build/couple/pair strategy for the synthesis of medium- and large-sized rings: discovery of macrocyclic histone deacetylase inhibitors. *J. Am. Chem. Soc.* **2010**, *132*, 16962–16976.
- (17) Vickers, C. J.; Olsen, C. A.; Leman, L. J.; Ghadiri, M. R. Discovery of HDAC inhibitors that lack an active site Zn<sup>2+</sup>-binding functional group. *ACS Med. Chem. Lett.* **2012**, *3*, 505–508.
- (18) Villadsen, J. S.; Kitir, B.; Wich, K.; Friis, T.; Madsen, A. S.; Olsen, C. A. An azumamide C analogue without the zinc-binding functionality. *MedChemComm* **2014**, *5*, 1849–1855.
- (19) Kuhn, B.; Fuchs, J. E.; Reutlinger, M.; Stahl, M.; Taylor, N. R. Rationalizing tight ligand binding through cooperative interaction networks. *J. Chem. Inf. Model.* **2011**, *51*, 3180–3198.
- (20) Hai, Y.; Christianson, D. W. Histone deacetylase 6 structure and molecular basis of catalysis and inhibition. *Nat. Chem. Biol.* **2016**, *12*, 741–747.
- (21) Porter, N. J.; Christianson, D. W. Structure, mechanism, and inhibition of the zinc-dependent histone deacetylases. *Curr. Opin. Struct. Biol.* **2019**, *59*, 9–18.
- (22) Jones, P.; Altamura, S.; Chakravarty, P. K.; Cecchetti, O.; De Francesco, R.; Gallinari, P.; Ingenito, R.; Meinke, P. T.; Petrocchi, A.; Rowley, M.; Scarpelli, R.; Serafini, S.; Steinkühler, C. A series of novel, potent, and selective histone deacetylase inhibitors. *Bioorg. Med. Chem. Lett.* **2006**, *16*, 5948–5952.
- (23) Jones, P.; Altamura, S.; De Francesco, R.; Paz, O. G.; Kinzel, O.; Mesiti, G.; Monteagudo, E.; Pescatore, G.; Rowley, M.; Verdirame, M.; Steinkühler, C. A novel series of potent and selective ketone histone deacetylase inhibitors with antitumor activity in vivo. *J. Med. Chem.* **2008**, *51*, 2350–2353.
- (24) Kinzel, O.; Llauger-Bufi, L.; Pescatore, G.; Rowley, M.; Schultz-Fademrecht, C.; Monteagudo, E.; Fonsi, M.; Paz, O. G.; Fiore, F.; Steinkühler, C.; Jones, P. Discovery of a potent class I selective ketone histone deacetylase inhibitor with antitumor activity in vivo and optimized pharmacokinetic properties. *J. Med. Chem.* **2009**, *52*, 3453–3456.
- (25) Yu, W.; Liu, J.; Yu, Y.; Zhang, V.; Clausen, D.; Kelly, J.; Wolkenberg, S.; Beshore, D.; Duffy, J.; Chung, C.; Myers, R. W.; Klein, D. J.; Fells, J.; Holloway, K.; Wu, J.; Wu, G.; Howell, B. J.; Barnard, R. J. O.; Kozlowski, J. Discovery of ethyl ketone-based HDACs 1, 2, and 3 selective inhibitors for HIV latency reactivation. *Bioorg. Med. Chem. Lett.* **2020**, *30*, 127197.
- (26) Pearson, R.; Kim, Y. K.; Hokello, J.; Lassen, K.; Friedman, J.; Tyagi, M.; Karn, J. Epigenetic silencing of human immunodeficiency virus (HIV) transcription by formation of restrictive chromatin structures at the viral long terminal repeat drives the progressive entry of HIV into latency. *J. Virol.* **2008**, *82*, 12291–12303.
- (27) Millard, C. J.; Watson, P. J.; Celardo, I.; Gordiyenko, Y.; Cowley, S. M.; Robinson, C. V.; Fairall, L.; Schwabe, J. W. R. Class I HDACs share a common mechanism of regulation by inositol phosphates. *Mol. Cell* **2013**, *51*, 57–67.
- (28) Watson, P. J.; Fairall, L.; Santos, G. M.; Schwabe, J. W. R. Structure of HDAC3 bound to co-repressor and inositol tetraphosphate. *Nature* **2012**, *481*, 335–340.
- (29) Moreno-Yruela, C.; Fass, D. M.; Cheng, C.; Herz, J.; Olsen, C. A.; Haggarty, S. J. Kinetic Tuning of HDAC Inhibitors Affords Potent Inducers of Progranulin Expression. *ACS Chem. Neurosci.* **2019**, *10*, 3769–3777.
- (30) Das, B.; Dobrowolski, C.; Shahir, A.-M.; Feng, Z.; Yu, X.; Sha, J.; Bissada, N. F.; Weinberg, A.; Karn, J.; Ye, F. Short chain fatty acids potently induce latent HIV-1 in T-cells by activating P-TEFb and multiple histone modifications. *Virology* **2015**, *474*, 65–81.
- (31) Nguyen, K.; Das, B.; Dobrowolski, C.; Karn, J. Multiple histone lysine methyltransferases are required for the establishment and maintenance of HIV-1 latency. *mBio* **2017**, *8*, e00133-17.